

Search for new massive resonances decaying to two charged leptons at CMS

T. REIS(*) on behalf of the CMS COLLABORATION

*Interuniversity Institute for High Energies, Université Libre de Bruxelles ULB
Boulevard du Triomphe 2, 1050 Brussels, Belgium*

ricevuto il 31 Luglio 2014

Summary. — A search for new massive bosons decaying to two charged leptons ($Z' \rightarrow l^+l^-$) with the dataset collected by the CMS experiment in 2012, corresponding to about 20 fb^{-1} of pp collisions at 8 TeV, is presented. In the absence of a significant deviation from the standard model predictions, upper limits on the new resonances production cross section times branching fraction are estimated. Furthermore, projections of the discovery potential for new heavy bosons decaying to two charged leptons for future runs of the LHC are shown.

PACS 2.60.Cn – Extensions of electroweak gauge sector.

PACS 14.70.Pw – Other gauge bosons.

1. – Introduction

There exist many theories beyond the standard model (SM) that predict the existence of heavy bosons, for example grand unified theories (GUT) [1] and theories with extra spatial dimensions [2]. The search for new massive bosonic resonances is one of the analysis types that profit heavily from the high proton-proton center-of-mass energies of the Large Hadron Collider (LHC) at CERN. If the new boson decays into electrons or muons, one is provided with a clear signature to search for new physics. A search for new resonances with a dileptonic decay, generally named Z' , was performed [3] with the Compact Muon Solenoid (CMS) experiment at the LHC using the dataset collected in 2012 from pp collisions at a center-of-mass energy of 8 TeV. The CMS detector is presented in sect. 2 and the analysis is discussed in sect. 3. A study of the discovery potential for future runs of the LHC was performed [4] for a center-of-mass energy of 14 TeV and is presented in sect. 4.

(*) E-mail: thomreis@ulb.ac.be

2. – The CMS detector

The main feature of the CMS detector [5] is a superconducting solenoid magnet with an internal diameter of 6 m, that generates an axial field of 3.8 T. Inside the solenoid are the silicon pixel and strip trackers, the crystal electromagnetic calorimeter (ECAL), and the brass/scintillator hadronic calorimeter (HCAL). Gas-ionisation muon detectors are located in between the layers of the iron return yoke outside the solenoid. The detector consists of a barrel part which houses the solenoid and is closed with two endcaps with forward calorimetry and muon detectors.

3. – Search for heavy resonances in the ee and $\mu\mu$ channels

The dataset for the analysis corresponds to an integrated luminosity of 19.6 fb^{-1} and 20.6 fb^{-1} , respectively for the dielectron and dimuon channels. The result is interpreted in the context of the Z'_{SSM} with SM like couplings of the sequential SM [6] and the Z'_ψ model coming from GUT [1].

3.1. Event selection. – Electron candidates are reconstructed from an energy deposit in the ECAL with an associated track in the tracker. In order to be selected they have to pass ID cuts, and fulfil isolation criteria for the track and ECAL/HCAL energy deposit to reject background coming from jets. Not more than one missing hit in the inner tracker is allowed for the track in order to reject electrons from photon conversions. The dielectron sample is obtained from events with two electron candidates with a transverse energy $E_T \geq 35 \text{ GeV}$ and at least one of them in the barrel region of the detector. The event has to be triggered by a double electron trigger with loose calorimeter and tracker ID criteria and an E_T threshold of 33 GeV . The analysis is done separately for events with one and two barrel electron(s), as the detector performs differently in the barrel and endcap regions.

Muon candidates are reconstructed from tracks in the inner tracker and the muon stations with hits in all subsystems. The tracks are reconstructed independently in the inner tracker and the muon stations and then matched to form a muon track that spans the complete detector. Isolation criteria are applied in order to reject background coming from jets. Cosmic muons are suppressed by the requirement for the track to have a small transverse impact parameter with respect to the primary vertex. The dimuon sample is obtained from events with two muons with opposite charge and with a transverse momentum $p_T \geq 45 \text{ GeV}$ coming from a common vertex. The event has to be triggered by a single muon trigger with a p_T threshold of 40 GeV and a pseudorapidity range $|\eta| < 2.1$. As one of the muons has to be matched to the trigger object, the pseudorapidity of this muon is limited to be smaller $|\eta| < 2.1$, while the second muon can have pseudorapidities up to $|\eta| = 2.5$. To further suppress cosmic muons the three dimensional angle between the tracks of the two muons has to be smaller than $\pi - 0.02$.

The efficiencies of the electron and muon identifications and isolations are measured with tag and probe techniques at the Z resonance peak for different regions of the detector, and amount to 88% (84%) for electrons in the barrel (endcap) region and 94% for muons.

3.2. Backgrounds. – After selection, the largest and irreducible background from SM processes is the Drell-Yan (DY) production (Z/γ^*) which is estimated from simulations. Reducible background, with events from $t\bar{t}$, tW , and diboson production also contributes. These events are taken from simulations as well and are validated with the so-called “electron-muon method” which looks at the invariant mass spectrum of events with $e\mu$

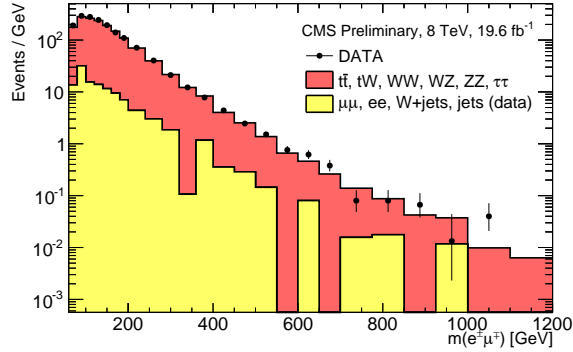


Fig. 1. – The observed opposite-sign $e^\pm\mu^\mp$ invariant-mass spectrum used for the validation of the prompt lepton invariant-mass spectrum.

pairs in the final state. This spectrum, after correcting for the different acceptances and efficiencies, should yield twice as many events for the reducible backgrounds from $t\bar{t}$, tW , and diboson production as the ee spectrum or the $\mu\mu$ spectrum. The opposite sign $e\mu$ invariant mass spectrum is shown in fig. 1. Background from multijet events is estimated from the same sign $e\mu$ invariant-mass spectrum as the difference between the data and the simulated backgrounds, and then used for the opposite sign $e\mu$ invariant-mass spectrum.

The background from misidentified jets is more important for the dielectron channel and is estimated from data by deriving a rate of jets from a jet enriched sample that pass the selection. This rate is then applied to a sample with two electron candidates that fail the selection. Contributions to the jet background from events with one real electron are added from simulated samples.

Background events coming from cosmic ray muons traversing the detector are effectively suppressed by the muon selection and are found to be negligible.

3.3. Results. – The invariant-mass spectra of the dielectron and dimuon channels are shown in fig. 2. The region around the Z resonance from 60 GeV to 120 GeV is used for the energy scale calibration, efficiency measurements and the normalisation of the

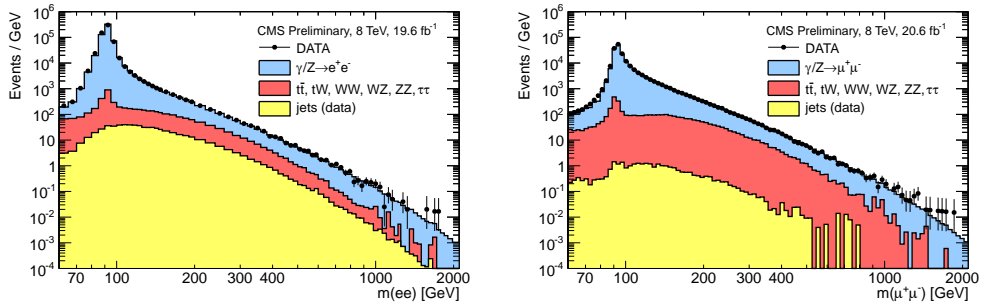


Fig. 2. – Invariant-mass spectra of the dielectron channel (left) and the dimuon channel (right).

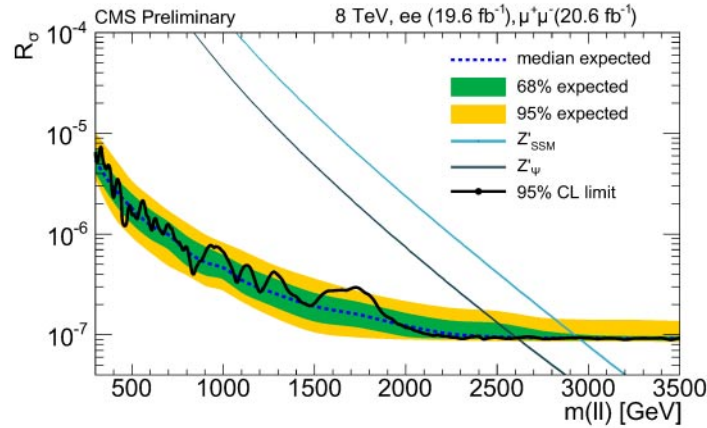


Fig. 3. – Combined upper limits at 95% CL on the ratio of cross section times branching ratio between a new heavy resonance and the Z resonance.

simulations. Above that, up to an invariant mass of 200 GeV, no new physics is expected and the region is used to verify the high mass behaviour of the analysis. The search region starts for invariant masses greater than 200 GeV. For the dielectron channel, the highest invariant-mass event selected is an event with two barrel electrons with a reconstructed invariant mass of $M_{ee} = 1776$ GeV. For the dimuon channel, an event with $M_{\mu\mu} = 1824$ GeV has the highest reconstructed invariant mass.

In the absence of an excess, limits are set on the ratio of cross section times branching ratio between a new heavy resonance and the Z resonance. Taking the ratio for the limit setting procedure cancels or suppresses several systematic uncertainties, notably the uncertainty on the luminosity which was 2.6% for the 2012 data taking period. A fully shape based Bayesian approach is used in order to obtain the limits for the assumption of a narrow resonance. The main systematics are uncertainties on the acceptance times efficiency (3–6%) and the mass dependent uncertainty on the background fit (2–20%). The limit for the combination of the barrel and endcap dielectron channels and the dimuon channel is shown in fig. 3. For two benchmark models, the Z'_{SSM} from the sequential SM, and the superstring inspired Z'_ψ , 95% confidence level (CL) lower limits on the resonance mass are derived. Masses below 2.96 TeV and 2.60 TeV can be excluded for the Z'_{SSM} and Z'_ψ models, respectively.

4. – Discovery potential for future runs

To estimate the discovery reach of the Z' searches for the upcoming run 2 of the LHC and beyond, studies are made with generator level simulations at a center-of-mass energy of 14 TeV. In absence of measurements at this energy, acceptances, efficiencies and resolutions are taken to be the same as for the 8 TeV run. The largest contribution to the background is irreducible and comes from Drell-Yan events. Background events coming from $t\bar{t}$ events self-veto for dilepton mass above about 1 TeV due to the fact that the top (antitop) quark is very boosted and its decay products, the b jet and the lepton are close to each other. The event is then rejected because the lepton fails the isolation criteria of the lepton selection. Above 1 TeV the WW background becomes the dominant reducible background. The background from misidentified jets is not taken into account for the study.

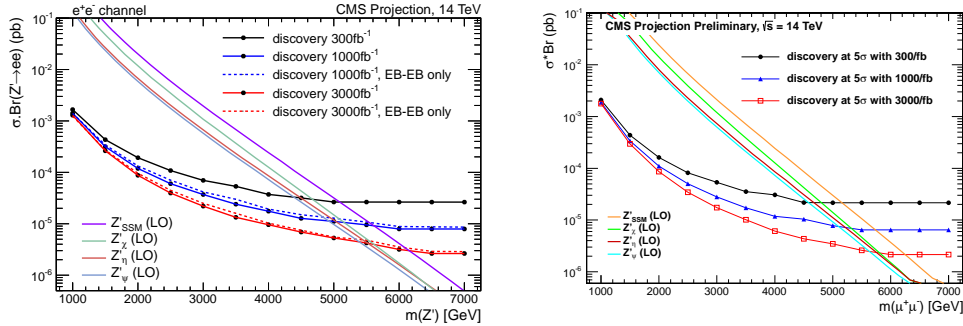


Fig. 4. – The minimum cross section times branching fraction for discovery of dielectron (left) and dimuon (right) mass for various luminosity scenarios. For the dielectron channel, “EB-EB only” represents a reduced acceptance scenario where electrons are only reconstructed in the ECAL barrel.

In the dielectron channel, the saturation of the ECAL readout electronics of a single crystal due to the high-energy deposit of an electron has to be taken into account. In the barrel region of the detector the saturation starts at energies greater than 1.7 TeV, and in the endcap at energies greater than 3 TeV. The loss of resolution due to the ECAL saturation is included in the study. Especially the endcap region of the ECAL will suffer from the high particle flux in the forward region and degrade over time. Thus, a reduced acceptance scenario is studied where the endcaps are not used for the analysis.

The projected discovery potential for the dielectron and dimuon channels is shown in fig. 4 for three different numbers of integrated luminosities. For 300 fb^{-1} , which corresponds to the expected integrated luminosity by the end of 2021, both, dielectron and dimuon channel can reach up to a mass of about 5 TeV for a 5σ discovery of a Z'_{SSM} .

* * *

The author is supported by the FNRS (Belgium) through its IISN program.

REFERENCES

- [1] LEIKE A., *Phys. Rep.*, **317** (1999) 143.
- [2] RANDALL L. and SUNDRUM R., *Phys. Rev. Lett.*, **83** (1999) 3370.
- [3] CMS COLLABORATION, *Search for Narrow Resonances in Dilepton Mass Spectra in pp Collisions at $\sqrt{s} = 8 \text{ TeV}$* , Public Analysis Summary, CMS-EXO-12-061.
- [4] CMS COLLABORATION, *Projected Performance of an Upgraded CMS Detector at the LHC and HL-LHC: Contribution to the Snowmass Process*, CMS-NOTE-13-002, arXiv:1307.7135.
- [5] CMS COLLABORATION, *JINST*, **3** (2008) S08004.
- [6] ALTARELLI G., MELE B. and RUIZ-ALTABA M., *Z. Phys. C*, **45** (1989) 109.